

Article

Induction of Senescence by Loss of *Gata4* in Cardiac Fibroblasts

Zhentao Zhang ^{1,2,*}, Gabriella Shayani ², Yanping Xu ¹, Ashley Kim ², Yurim Hong ², Haiyue Feng ² and Hua Zhu ^{1,*} 

¹ Department of Surgery, Davis Heart and Lung Research Institute, The Ohio State University Wexner Medical Center, Columbus, OH 43210, USA; yanping.xu@osumc.edu

² Division of Cardiovascular Medicine, Department of Medicine, Vanderbilt University Medical Center, Nashville, TN 37232, USA; gabriella.i.shayani@vanderbilt.edu (G.S.); ashley.h.kim@vanderbilt.edu (A.K.); yurim.hong@vanderbilt.edu (Y.H.); haiyue.feng@vumc.org (H.F.)

* Correspondence: zhentao.zhang@osumc.edu (Z.Z.); hua.zhu@osumc.edu (H.Z.)

Abstract: Cardiac fibroblasts are a major source of cardiac fibrosis during heart repair processes in various heart diseases. Although it has been shown that cardiac fibroblasts become senescent in response to heart injury, it is unknown how the senescence of cardiac fibroblasts is regulated in vivo. *Gata4*, a cardiogenic transcription factor essential for heart development, is also expressed in cardiac fibroblasts. However, it remains elusive about the role of *Gata4* in cardiac fibroblasts. To define the role of *Gata4* in cardiac fibroblasts, we generated cardiac fibroblast-specific *Gata4* knockout mice by cross-breeding *Tcf21-MerCreMer* mice with *Gata4^{fl/fl}* mice. Using this mouse model, we could genetically ablate *Gata4* in *Tcf21* positive cardiac fibroblasts in an inducible manner upon tamoxifen administration. We found that cardiac fibroblast-specific deletion of *Gata4* spontaneously induces senescence in cardiac fibroblasts in vivo and in vitro. We also found that *Gata4* expression in both cardiomyocytes and non-myocytes significantly decreases in the aged heart. Interestingly, when α MHC-*MerCreMer* mice were bred with *Gata4^{fl/fl}* mice to generate cardiomyocyte-specific *Gata4* knockout mice, no senescent cells were detected in the hearts. Taken together, our results demonstrate that *Gata4* deficiency in cardiac fibroblasts activates a program of cellular senescence, suggesting a novel molecular mechanism of cardiac fibroblast senescence.

Keywords: senescence; fibroblast; *Gata4*; heart; *Tcf21*



Citation: Zhang, Z.; Shayani, G.; Xu, Y.; Kim, A.; Hong, Y.; Feng, H.; Zhu, H. Induction of Senescence by Loss of *Gata4* in Cardiac Fibroblasts. *Cells* **2023**, *12*, 1652. <https://doi.org/10.3390/cells12121652>

Academic Editor: Wayne Carver

Received: 26 April 2023

Revised: 6 June 2023

Accepted: 13 June 2023

Published: 17 June 2023



Copyright: © 2023 by the authors. Licensee MDPI, Basel, Switzerland. This article is an open access article distributed under the terms and conditions of the Creative Commons Attribution (CC BY) license (<https://creativecommons.org/licenses/by/4.0/>).

1. Introduction

Cardiac fibroblasts are a major cellular population that regulates extracellular matrix (ECM) production and cardiac fibrosis [1,2]. In response to cardiac injury, cardiac fibroblasts become activated and differentiate into myofibroblasts. The resulting myofibroblasts are the primary source of the extracellular matrix. Excessive extracellular matrix deposition in response to heart injury leads to cardiac fibrosis. Although cardiac fibrosis is initially an adaptive response, its progression disrupts the mechanical architecture of the heart and thus leads to adverse remodeling and heart failure [3,4]. Therefore, extensive studies have focused on the differentiation of cardiac fibroblasts in the context of heart injury. However, much less is known about how the homeostasis of cardiac fibroblasts is regulated in vivo.

Cellular senescence is a programmed cell cycle arrest that prevents the proliferation of old, damaged, and potentially tumorigenic cells [5–7]. As such, cellular senescence was initially recognized as a potent tumor-suppressive mechanism that arrests the growth of cells at risk for malignant transformation. However, numerous recent studies identified diverse roles of cellular senescence in the context of physiological or pathological processes beyond tumor suppression [5–8]. Importantly, cellular senescence has been shown to play important roles in fibrotic wound repair processes in multiple tissues, including the liver [9], skin [10,11], lung [12], heart [13–16], and spinal cord [17]. It has been shown that activated cardiac fibroblasts or myofibroblasts become senescent in response to heart injuries [13–15].

It was demonstrated that senescence of activated cardiac fibroblasts or myofibroblasts is significantly decreased in the global p53 or p53/p16 double knockout mouse model, indicating that senescence of these cardiac fibroblast-derived cells is mediated by p53 and/or p16 pathways [13,14]. These studies also suggested that inhibition of senescence by inactivating p53 or both p16 and p53 increases cardiac fibrosis. In contrast, a recent study showed that eliminating senescent cells using synolytics can decrease scar formation and improve heart function after ischemia-reperfusion injury [16]. Therefore, although the precise roles of cellular senescence during heart injury need to be further investigated, it becomes clear that the senescence of cardiac fibroblast-derived cells (i.e., activated cardiac fibroblasts and myofibroblasts) is involved in heart repair processes. However, it remains elusive about the molecular regulation of senescence of cardiac fibroblasts.

Gata4, one of the earliest genes expressed during heart development, plays critical roles in cardiomyocyte proliferation, differentiation, survival, and hypertrophy [18–26]. Although *Gata4*'s roles in the heart have been exclusively studied for cardiomyocytes, it has been shown that *Gata4* mRNA and protein level in isolated cardiac fibroblasts is comparable to or even higher than that in the whole heart of adult mice [27,28]. In contrast, *Gata4* expression was very low in tail-tip or skin fibroblasts, suggesting that *Gata4* abundance in fibroblasts is cardiac-specific [27,28]. A recent study has suggested that *Gata4*, together with *Gata6* in periostin lineage traced cells (i.e., activated cardiac fibroblasts and myofibroblasts), contributes to enhancing angiogenesis in a pressure overload mouse model [29]. However, *Gata4*'s role in cardiac fibroblast homeostasis is still unknown.

In this study, we sought to determine the role of *Gata4* in cardiac fibroblasts using a cardiac fibroblast-specific, inducible *Gata4* knockout mouse model. We found that loss of *Gata4* in cardiac fibroblasts induces senescence without heart injury. In addition, the role of *Gata4* in cellular senescence seems to be cardiac fibroblast specific, as cellular senescence was not observed in the heart of a cardiomyocyte-specific, inducible *Gata4* knockout mouse model. Our results suggest that *Gata4* may be an important gatekeeper for the cellular senescence of cardiac fibroblasts. Thus, it might be a potential target to treat cardiac fibrosis.

2. Materials and Methods

2.1. Mice

All studies conformed with the principles of the National Institutes of Health “Guide for the Care and Use of Laboratory Animals”, (NIH publication No. 85-12, revised 1996). The mice were given unrestricted access to food and water and were housed under a 12 h light/dark cycle at a consistent room temperature of 24 ± 2 °C, with a steady humidity of $40 \pm 15\%$. *Tcf21^{iCre}:R26R^{tdT}* and *Tcf21^{iCre}:Gata4^{fl/fl}* mice were generated by cross-breeding *Tcf21^{iCre}* [30,31] with Rosa26-CAG-loxP-Stop-loxP-tdTomato mice (Jackson Laboratory, Bar Harbor, ME, USA) and *Gata4^{fl/fl}* mice [32], respectively. Subsequently, *Tcf21^{iCre}:Gata4^{fl/fl}:R26R^{tdT}* mice were generated by cross-breeding *Tcf21^{iCre}:R26R^{tdT}* mice with *Gata4^{fl/fl}* mice. *α MHC^{iCre}:Gata4^{fl/fl}* mice were generated by cross-breeding *α MHC^{iCre}* mice (The Jackson Laboratory) with *Gata4^{fl/fl}* mice. In this study, 7-week-old and 72-week-old male and female mice were used for the experiments. Tamoxifen (Sigma) was dissolved in corn oil at a concentration of 10 mg/mL by shaking overnight at 37 °C with light protection. To induce Cre activity, tamoxifen was administered to the mice via intraperitoneal injection for 5 consecutive days (75 mg/kg for *Tcf21^{iCre}* and 40 mg/kg for *α MHC^{iCre}*). 8-weeks and 72-week-old C57BL6 mice were obtained from the Jackson Laboratory. Carbon dioxide (CO₂) inhalation was used as a primary euthanasia, followed by cervical dislocation as a secondary measure.

2.2. Immunohistochemistry

After the hearts were washed with ice-cold PBS, they were fixed with pre-chilled 4% paraformaldehyde (PFA) in PBS overnight at 4 °C and then incubated in 30% sucrose in PBS on a rotary shaker overnight at 4 °C. The fixed hearts were embedded in O.C.T compound and frozen in pre-chilled isopentane with liquid nitrogen. The frozen hearts

were sectioned at 8 μm thickness. After 10 min of air drying, the heart sections were washed with PBS three times and then fixed again with pre-chilled 4% PFA in PBS on ice for 20 min. After PBS washes thrice, the fixed heart sections were permeabilized in 0.1% Triton X-100 in PBS for 20 min. The heart sections were washed three times with PBS and then blocked with M.O.M mouse IgG blocking reagent (Vector Labs, Newark, CA, USA) for 1 h and 5% donkey serum in M.O.M protein diluent (Vector Labs) for 30 min at room temperature. The heart sections were incubated with anti-Troponin I (Abcam, Waltham, MA, USA, cat# ab188877, 1:400 dilution), anti-Gata4 (ThermoFisher, Waltham, MA, USA, cat# PA1-102, 1:200 dilution), anti-p16 (Santa Cruz, Dallas, TX, USA, cat# sc56330, 1:200 dilution), or indicated combinations of the primary antibodies for 1 h at room temperature. After the heart sections were washed with PBS three times, they were incubated with AlexaFluor secondary antibodies (ThermoFisher) for one hour at room temperature and mounted with Vectashield antifade mounting medium with DAPI (VectorLabs, Newark, CA, USA, cat# H-2000). tdTomato was visualized without immunostaining. For wheat germ agglutinin (WGA) staining, the heart sections were incubated with WGA staining solution (ThermoFisher, cat# W32464) prepared per manufacturer's instruction, along with secondary antibodies. Images were captured using Zeiss LSM 880 confocal microscope or Olympus IX81 epifluorescent microscope. A total of 6 heart sections per mouse were used for quantification. Fluorescent pictures of four randomly selected fields per section were captured and analyzed by MetaExpress software (Molecular Device, San Jose, CA, USA) in an automated manner.

2.3. Senescence-Associated β -Galactosidase (SA β -Gal) Staining

Cryo-embedded heart sections were prepared as described above and stained using a SA β -gal staining kit (Sigma, Setagaya city, Japan, cat# CS0030-1KT) per the manufacturer's protocol. Briefly, frozen heart sections were fixed with 4% PFA for 10 min at room temperature and washed thrice with PBS. The heart sections were incubated with freshly prepared SA β -gal staining solution (per the kit's instruction) overnight at 37 °C. After stained heart sections were washed with PBS thrice, the pictures were captured using Leica DMIL LED, $n = 5$.

2.4. Isolation of Non-Myocytes Using Langendorff Perfusion

Adult mouse hearts were dissected and perfused retrogradely via aortic cannulation in a Langendorff apparatus as described previously [33]. The dissected hearts were serially perfused with perfusion buffer (NaCl 120.4 mM, KCl 14.7 mM, Na_2HPO_4 0.6 mM, K_2HPO_4 0.6 mM, MgSO_4 1.2 mM, Na-HEPES 10 mM, NaHCO_3 4.6 mM, Taurine 30 mM, BDM 10 mM, Glucose 5.5 mM, pH 7.0), digestion buffer without CaCl_2 (Collagenase II 2.4 mg/mL in perfusion buffer), and digestion buffer with CaCl_2 (Collagenase II 2.4 mg/mL, and CaCl_2 40 μM in perfusion buffer). The perfused hearts were displaced from the Langendorff apparatus. Ventricular cardiomyocytes were mechanically dissociated and triturated using a fine scalpel and scissors and resuspended in stopping buffer (CaCl_2 11.7 μM in calf serum 2 mL plus perfusion buffer 18 mL). Cells were centrifuged at a low speed, and the supernatant was collected as a non-myocyte population. The supernatant was centrifuged at $350 \times g$ for 10 min to obtain non-myocytes, $n = 3$.

2.5. Neonatal Cardiac Fibroblast Isolation

Neonatal cardiac fibroblasts were isolated using the Neomyts kit (Cellutron, Baltimore, MD, USA, cat# nc-6031). Following the digestion of the hearts per the manufacturer's protocol, we harvested cells containing a mix of cardiomyocytes and cardiac fibroblasts. These mixed cells were then plated in a 6-well plate and allowed to settle for 40 min, enabling the cardiac fibroblasts to attach to the bottom. The supernatant, which contains cardiomyocytes, was discarded. The cells were subsequently cultured in Dulbecco's Modified Eagle's Medium (DMEM) (Gibco, Grand Island, NY, USA, cat# 10564011), supplemented with 10% fetal bovine serum (FBS) (Corning, New York, NY, USA, cat# 35-070-CV) and 1% penicillin-streptomycin (Sigma, P0781).

2.6. Adenovirus Infection

Non-myocytes isolated using Langendorff perfusion described above were plated into a 10 cm culture dish. Mostly cardiac fibroblasts were attached to the culture dish. Cardiac fibroblasts were cultured until they reached ~70–80% confluency. Then, cardiac fibroblasts were trypsinized, replated into a 24-well plate, and then infected with Ad-vector (Ad5CMVempty, VVC-U of Iowa-272) or Ad-Cre (Ad5-CMV-Cre, VVC-U of Iowa-5) viruses purchased from the University of Iowa Viral Core following the core's Adenovirus infection protocol (www.medicine.uiowa.edu/vectorcore (accessed on 12 November 2020)).

2.7. Immunocytochemistry

After cells were fixed with 4% paraformaldehyde for 15 min, they were washed with permeabilization buffer (0.05% Triton-X in PBS) for 5 min three times at room temperature. The fixed cells were incubated with blocking buffer (BiogeneX, Fremont, CA, USA, cat# HK085) for 45 min, and then incubated with primary antibodies against Gata4 (Thermo Scientific, Waltham, MA, USA, cat# PA1-102, 1:400 dilution), Ki67 (Abcam, cat# ab92742, 1:1000 dilution), α SMA (Sigma, cat# A5228, 1:1000 dilution), or γ H2AX (Novus Biologicals, Centennial, CO, USA, cat#NB100-384, 1:200) overnight at 4 °C. After being washed with permeabilization buffer three times for 5 min, cells were incubated with Alexa fluorogenic secondary antibodies (ThermoFisher) at 1:400 dilution at room temperature for 1 h. For each animal, five slides ranging from the top to the bottom of the heart were selected for staining. Cells were rewashed with permeabilization buffer three times and then incubated with DAPI solution at a final concentration of 2 μ M in permeabilization buffer for 15 min. After cells were washed three times with permeabilization buffer, cell images were captured with ImageXpress Micro XL Automated Cell Imaging system (Molecular Device), $n = 3$.

2.8. EdU Incorporation Assay

EdU incorporation assay was performed using Click-iT Plus EdU imaging kit (Thermo Fisher, cat# C10637) per the manufacturer's protocol. Briefly, cardiac fibroblasts were cultured in a fibroblast growth medium supplemented with 10 μ M EdU for 24 h. After cells were fixed with 4% paraformaldehyde for 15 min, they were washed with 3% BSA in PBS twice at room temperature. The fixed cells were permeabilized with 0.5% Triton-X in PBS for 20 min at room temperature and then incubated with freshly prepared EdU staining solution (as per kit's instruction) for 30 min with light protection, $n = 3$.

2.9. High Content Imaging and Analysis

High-content imaging analysis was performed as described previously [34–37]. The images of immunostained cells were acquired with a 10 \times objective at 36 fields per well using ImageXpress Micro XL Automated Cell Imaging system (Molecular Device) using DAPI and Texas Red or FITC filter sets. The number of Texas Red or FITC fluorescent positive cells among DAPI fluorescent positive cells was quantified using MetaXpress software (Molecular Device), $n = 5$.

2.10. Echocardiography

Echocardiographic imaging was performed by skilled technicians at the Vanderbilt Cardiovascular Physiology Core using the Visual Sonics Vevo 2100 small animal imaging system. Mice were lightly anesthetized using 1.5% isoflurane and placed supine on a heating pad. Parasternal short-axis M-mode imaging was used to visualize LV structure and function for the heart cycle.

2.11. FACS

Non-myocytes were isolated from $Tcf21^{iCre}:Gata4^{fl/fl}:R26R^{tdT}$, $Tcf21^{iCre}:R26R^{tdT}$, or wild-type mice using Langendorff perfusion as described above. tdTomato⁺ cells were sorted on FACSaria III (BD Biosciences). The gate for tdTomato⁺ cells was set using tdTomato⁻ cells

isolated from wild-type mice. Sorted tdTomato⁺ cells were used for qPCRs to determine the mRNA expression level of *Gata4*, $n = 3$.

2.12. Quantitative Real-Time PCR (qPCR)

Total RNA was isolated from sorted tdTomato⁺ cells using NucleoSpin RNA Kit (Macherey-Nagel). cDNA was synthesized by reverse transcription qPCR using High-Capacity cDNA Reverse Transcription Kit (Applied Biosystems, Waltham, MA, USA, cat# 4368814). qPCR analyses were performed using SYBR probes and iTaq Universal SYBR Green Supermix (Bio-Rad, Hercules, CA, USA, cat# 1725121) on a Bio-Rad CFX96 system (Bio-Rad). The gene expression level was normalized to GAPDH.

2.13. Statistical Analyses

Statistical significance was determined using unpaired two-tailed Student's t-test between two groups or one-way ANOVA with Tukey's post hoc analysis among three groups. p -values of < 0.05 were regarded as significant. GraphPad Prism 8 was used for data visualization and statistical analysis.

3. Results

In previous studies, *Gata4* is known to be expressed in cardiac fibroblasts [27,28]. Its expression level in cardiac fibroblasts was much higher than the fibroblasts derived from other organs and surprisingly even higher than that in the whole adult mouse heart [27]. Given the heterogeneous nature of cardiac fibroblasts, we sought to precisely determine *Gata4* expression in cardiac fibroblasts using cardiac fibroblast lineage reporter mice that were generated by cross-breeding *Tcf21-MerCreMer* mice with *Rosa26-CAG-loxP-Stop-loxP-tdTomato* mice (referred to as *Tcf21^{iCre}:R26R^{tdT}* mice). *Tcf21*, an epicardial transcription factor, is expressed in epicardium-derived cardiac fibroblasts, constituting more than 80% of cardiac fibroblasts in the heart [38,39]. In *Tcf21^{iCre}:R26R^{tdT}* mice, cardiac fibroblasts are specifically labeled with tdTomato upon tamoxifen administration [30]. A week after tamoxifen administration, we processed heart sections and performed immunostaining for *Gata4*. We identified *Gata4*⁺tdTomato⁺ *Tcf21* lineage traced cells (Figure 1A). Our results showed that *Gata4* indeed expresses in *Tcf21* lineage traced cardiac fibroblasts.

To investigate the role of *Gata4* in cardiac fibroblasts, we generated inducible, cardiac fibroblast-specific *Gata4* knockout mice by cross-breeding *Tcf21-MerCreMer* mice with *Gata4^{fl/fl}* mice (referred to as *Tcf21^{iCre}:Gata4^{fl/fl}* mice) (Figure 1B). We also generated *Tcf21^{iCre}:Gata4^{fl/fl}:R26R^{tdT}* mice by cross-breeding *Tcf21^{iCre}:R26R^{tdT}* mice with *Gata4^{fl/fl}* mice to identify *Gata4* deficient cardiac fibroblasts with tdTomato expression. This conditional knockout approach bypasses the embryonic lethality caused by germline *Gata4* deficiency [21,24] and thus allows us to study the effect of *Gata4* loss in adult cardiac fibroblasts. Using these mouse models, we could genetically ablate *Gata4* in an inducible manner upon tamoxifen administration. A week after administering tamoxifen into *Tcf21^{iCre}:R26R^{tdT}* (control) and *Tcf21^{iCre}:Gata4^{fl/fl}:R26R^{tdT}* mice for 5 consecutive days, we processed frozen heart sections and immunostained for *Gata4*. While *Gata4* was frequently expressed in tdTomato⁺ cells in *Tcf21^{iCre}:R26R^{tdT}* mice, tdTomato⁺ cells rarely expressed *Gata4* in *Tcf21^{iCre}:Gata4^{fl/fl}:R26R^{tdT}* mice (Figure 1C,D). We also quantified the extent of genetic deletion of *Gata4* in *Tcf21* lineage-traced cells using qPCR (Figure 1E). After isolating non-myocytes from *Tcf21^{iCre}:R26R^{tdT}* (control) and *Tcf21^{iCre}:Gata4^{fl/fl}:R26R^{tdT}* mice, we sorted out tdTomato⁺ cells using fluorescence-activated cell sorting (FACS) (Figure S2). Using the sorted tdTomato⁺ cells from control and *Tcf21^{iCre}:Gata4^{fl/fl}:R26R^{tdT}* mice, we performed qPCR to assess the *Gata4* mRNA level. We found ~80% reduction of *Gata4* mRNA level in *Tcf21^{iCre}:Gata4^{fl/fl}:R26R^{tdT}* mice compared to that in *Tcf21^{iCre}:R26R^{tdT}* mice (Figure 1E). Taken together, our results demonstrated that our conditional *Gata4* knockout model efficiently inactivates *Gata4*, specifically in cardiac fibroblasts in vivo.

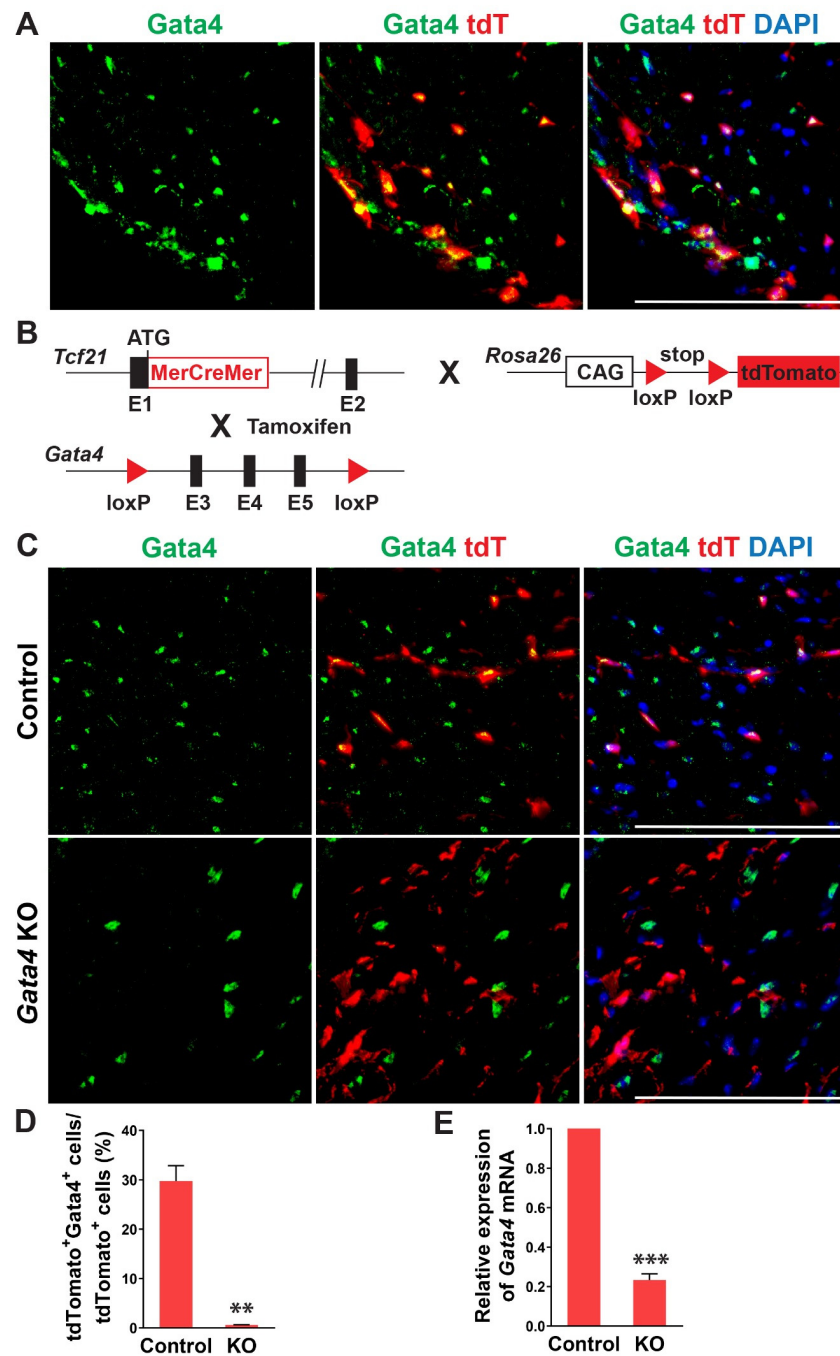


Figure 1. Gata4 expression and inactivation in Tcf21 lineage traced cardiac fibroblasts. (A) Gata4 expression in Tcf21 lineage traced cardiac fibroblasts. Following tamoxifen administration, 8-weeks old *Tcf21^{iCre}:R26R^{tdT}* mouse hearts were harvested, and heart sections were processed and immunostained for Gata4. Scale bar, 100 μ M. (B) Schematic illustration of generation of cardiac fibroblast specific, inducible *Gata4* knockout mice. *Tcf21^{iCre}* mice in which *MerCreMer* cDNA cassette was inserted into exon 1 (E1) were crossed with *Gata4* floxed mice which contain a pair of loxP sites encompassing exons 3, 4, and 5 (E3, 4, and 5) of *Gata4*. Alternatively, *Tcf21^{iCre}:R26R^{tdT}* mice were crossed with *Gata4* floxed mice. Activated *MerCreMer* by tamoxifen administration recombines two loxP sites to delete exons 3, 4, and 5 of *Gata4*, thereby inactivating *Gata4* in Tcf21 lineage traced cardiac fibroblasts. (C) Immunofluorescent analysis to demonstrate *Gata4* inactivation in Tcf21 lineage traced cardiac fibroblasts. Following tamoxifen administration, *Tcf21^{iCre}:R26R^{tdT}* (Control) and *Tcf21^{iCre}:Gata4^{fl/fl}:R26R^{tdT}* (*Gata4* KO) mouse hearts were harvested, and heart sections were processed and immunostained for Gata4. Scale bar, 100 μ M. (D) Quantification of Gata4 expressing

cardiac fibroblasts using immunostained heart sections from *Tcf21^{iCre}:R26R^{tdT}* (Control) and *Tcf21^{iCre}:Gata4^{fl/fl}:R26R^{tdT}* (KO) mice. The percentage of Gata4⁺tdTomato⁺ cells among tdTomato⁺ cells (Tcf21 lineage traced cardiac fibroblasts) was quantified. Three independent experiments are presented as mean \pm s.d. $n = 3$, ** $p < 0.01$. (E) qPCR analysis for *Gata4* mRNA level using sorted tdTomato⁺ cells from *Tcf21^{iCre}:Gata4^{fl/fl}:R26R^{tdT}* (KO). FACS-sorted tdTomato⁺ cells from *Tcf21^{iCre}:R26R^{tdT}* (Control) mice were used as control. Three independent experiments are presented as mean \pm s.d. $n = 3$, *** $p < 0.0001$.

Given *Gata4*'s positive regulation of cell cycle progression in highly proliferating, multiple different cell types [40–47], we tested if cardiac fibroblast-specific deletion of *Gata4* can induce senescence in quiescent cardiac fibroblasts in the heart. We administered tamoxifen to *Tcf21^{iCre}* (control) and *Tcf21^{iCre}:Gata4^{fl/fl}* mice for 5 consecutive days. Two or seven weeks after the completion of tamoxifen administration, we processed frozen heart sections and stained them for senescence-associated β -gal (SA β -gal) to evaluate cellular senescence. Surprisingly, we found a significant number of SA β -gal⁺ interstitial cells in *Tcf21^{iCre}:Gata4^{fl/fl}* mouse hearts, while nearly no senescent cells were observed in control hearts (Figure 2A,C). We also confirmed this result by immunostaining for p16, a widely used senescent marker [48]. P16, another senescent marker, was consistently markedly increased in *Tcf21^{iCre}:Gata4^{fl/fl}* mouse hearts compared to control hearts (Figure 2B,D). Lack of senescence in *Tcf21^{iCre}* control hearts excludes the possibility that Cre toxicity could induce senescence. Our results showed that specific deletion of *Gata4* in cardiac fibroblasts spontaneously induces cellular senescence in the heart in vivo. These findings suggest that *Gata4* may play a role in the regulation of cellular senescence in quiescent cardiac fibroblasts, while it contributes to cell proliferation in highly proliferative cells, including embryonic cardiomyocytes and intestinal epithelial cells and cancer cells [40,41,44–47].

To determine whether senescence induced by cardiac fibroblast-specific *Gata4* loss in the heart could be observed at the cellular level in a cell-autonomous manner, we also tested if loss of *Gata4* in isolated primary cardiac fibroblasts can result in senescence induction in vitro. We isolated adult cardiac fibroblasts from *Gata4^{fl/fl}* mice. To genetically delete *Gata4* in isolated cardiac fibroblasts, isolated *Gata4^{fl/fl}* cardiac fibroblasts were infected with a Cre-expressing adenovirus (Ad-Cre) or control adenovirus (Ad-vector). Three days after the adenoviral infection, we showed efficient *Gata4* inactivation in Ad-Cre infected cells (Figure 3A). We rarely observed *Gata4* expressing cells with Ad-Cre infection, while most cells expressed *Gata4* with Ad-vector infection. Using this cell-based *Gata4* knockout model, we first examined cell proliferation using EdU labeling and Ki67 immunostaining. Since senescent cells are withdrawn from the cell cycle, cellular senescence inversely correlates with cell proliferation rate. We found that both EdU⁺ and Ki67⁺ cells were significantly decreased by Ad-Cre infection, compared with Ad-vector infection, indicating that cell proliferation rate is reduced by the loss of *Gata4* in isolated cardiac fibroblasts (Figure 3B). Next, we performed SA β -gal staining 10 days after infecting Ad-Cre or Ad-vector into *Gata4^{fl/fl}* cardiac fibroblasts. We observed markedly increased SA β -gal⁺ cells by Ad-Cre infection, compared to Ad-vector infection (Figure 3C). As parallel experiments, we performed SA β -gal staining on wild-type cardiac fibroblasts infected with Ad-Cre. In contrast to *Gata4^{fl/fl}* cardiac fibroblasts infected with Ad-Cre, these cells did not show an appreciable increase in the percentage of senescent cells over the background level. These results indicate that senescence induction is indeed due to the loss of *Gata4* rather than a non-specific Cre toxicity. In addition, we immunostained the cells infected with Ad-Cre or Ad-vector for γ H2AX, a senescence marker. As expected, we found that significantly increased γ H2AX⁺ cells in *Gata4* deficient cells (Ad-Cre infected) than control cells (Ad-vector infected) (Figure 3C). We also use p16, another senescence marker, for the staining (Figure S3). Taken together, our results demonstrated that loss of *Gata4* induces senescence in isolated cardiac fibroblasts in vitro, suggesting that induction of cellular senescence by *Gata4* loss is a cell-autonomous effect.

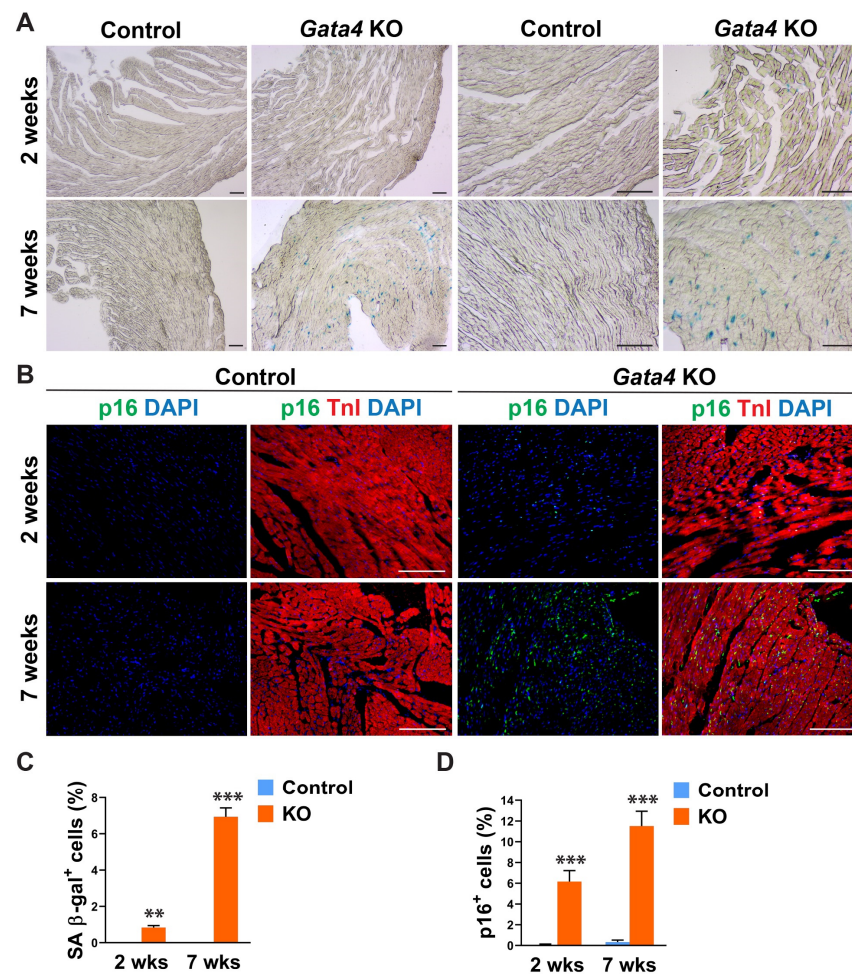


Figure 2. Senescence induction by Gata4 loss in cardiac fibroblasts in the heart. (A) Demonstration of senescence by SA β -gal staining. SA β -gal staining was performed on heart sections 2- or 7 weeks following tamoxifen administration into *Tcf21^{iCre}:Gata4^{fl/fl}* (Gata4 KO) or *Tcf21^{iCre}* (Control) mice. Scale bar, 40 μ M, and 100 μ M. (B) Demonstration of senescence by p16 immunostaining. The heart sections from *Tcf21^{iCre}:Gata4^{fl/fl}* (Gata4 KO) and *Tcf21^{iCre}* (Control) mice were immunostained for p16 2-week (2 wks) or 7-week (7 wks) following tamoxifen administration. Scale bar, 100 μ M. (C,D) Summary of quantification of senescent cells in cardiac fibroblast specific Gata4 deficient hearts. Three independent experiments are presented as mean \pm s.d. $n = 3$, ** $p < 0.01$; *** $p < 0.001$.

We examined the temporal expression pattern of Gata4 in the heart using mice of different ages. Interestingly, we found that the number of Gata4-expressing cells, including both cardiomyocytes and non-myocytes, is significantly decreased in the old mouse hearts (Figure S1). While Gata4 expression was robust in the neonatal heart, it was sparsely expressed in the 72 weeks old mouse heart. To determine if Gata4 in cardiomyocytes also plays a role in the repression of senescence, we generated cardiomyocyte-specific, inducible Gata4 knockout mice by cross-breeding α MHC-*MerCreMer* mice [49] with *Gata4^{fl/fl}* mice (referred to as α MHC^{iCre}:*Gata4^{fl/fl}*) (Figure 4A). Following tamoxifen administration, we could genetically ablate Gata4, specifically in cardiomyocytes. Nearly no Gata4 expressing cardiomyocyte was observed in α MHC^{iCre}:*Gata4^{fl/fl}* mice, while Gata4 was frequently expressed in cardiomyocytes of α MHC^{iCre} (control) mice (Figure 4B). However, Gata4⁺ interstitial cells were similarly found in both α MHC^{iCre}:*Gata4^{fl/fl}* and α MHC^{iCre} (control) mice. We found that the total number of Gata4⁺ cells is significantly reduced in α MHC^{iCre}:*Gata4^{fl/fl}* mouse hearts as opposed to α MHC^{iCre} (control) mouse hearts (Figures 4C and S4). Collectively, our data demonstrated that we could inactivate Gata4 specifically in cardiomyocytes in an inducible manner using the α MHC^{iCre}:*Gata4^{fl/fl}* mouse model. Next, we examined

senescence induction using SA β -gal staining and p16 immunostaining 7 weeks after tamoxifen administration into α MHC^{iCre}:*Gata4*^{fl/fl} and α MHCiCre mice. In contrast to cardiac fibroblast-specific *Gata4* knockout mice (Figure 2), we observed nearly no senescent cells in α MHC^{iCre}:*Gata4*^{fl/fl} mouse hearts in which *Gata4* was specifically lost in cardiomyocytes (Figure 4D,E). The transthoracic echocardiogram results reveal no reduction in contractile function in the hearts of cardiomyocyte-specific *Gata4* knockout mice (Figure S5). These results suggest that *Gata4*'s role in senescence inhibition is specific to cardiac fibroblasts.

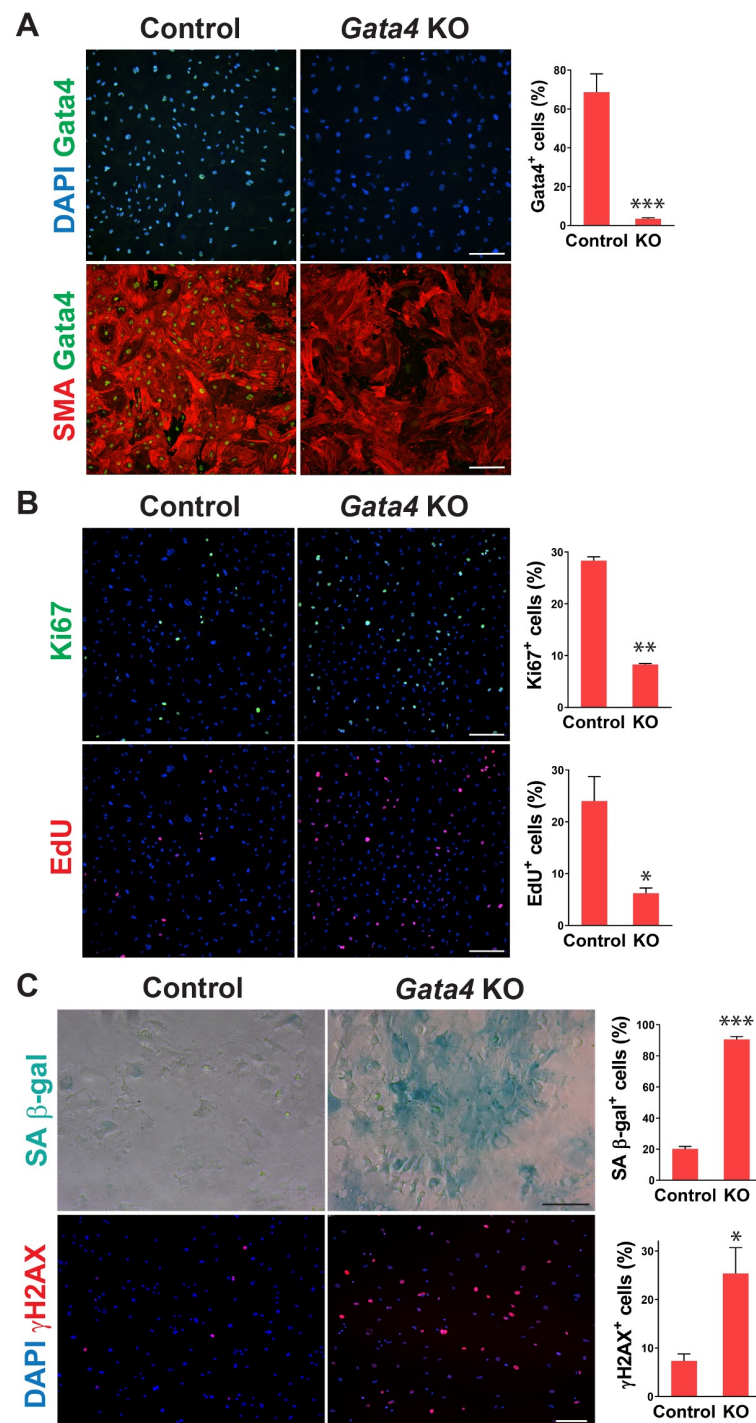


Figure 3. Senescence induction in *Gata4* deficient cardiac fibroblasts in vitro. (A) Inactivation of *Gata4* in vitro. Ad-Cre or Ad-vector viruses were infected into adult cardiac fibroblasts isolated from

Gata4^{fl/fl} mice. The infected cells were immunostained for alpha-smooth muscle actin (SMA) and Gata4. Representative immunofluorescent images of cells infected with Ad-vector (Control) or Ad-Cre (*Gata4* KO) were shown. Gata4-expressing cells were quantified using high-content imaging analysis. Five independent experiments are presented as mean \pm s.d. $n = 5$, *** $p < 0.0001$. Scale bar, 200 μ M. (B) The proliferation of Gata4 deficient cardiac fibroblasts. *Gata4^{fl/fl}* cardiac fibroblasts infected with Ad-vector (Control) or Ad-Cre (*Gata4* KO) were EdU labeled or immunostained for Ki67. Representative immunofluorescent images used for high-content imaging analysis were shown. Three independent experiments are presented as mean \pm s.d. $n = 3$, * $p < 0.05$; ** $p < 0.005$. Scale bar, 200 μ M. (C) Demonstration of senescence in Gata4 deficient cardiac fibroblasts. *Gata4^{fl/fl}* cardiac fibroblasts infected with Ad-vector (Control) or Ad-Cre (*Gata4* KO) were stained for SA β -gal or immunostained for γ H2AX. Representative SA β -gal stained or immunofluorescent images were shown. Five (for SA β -gal) and three (for γ H2AX) independent experiments are presented as mean \pm s.d. $n = 5$, * $p < 0.05$; $n = 3$, *** $p < 0.0001$. Scale bar, 100 μ M.

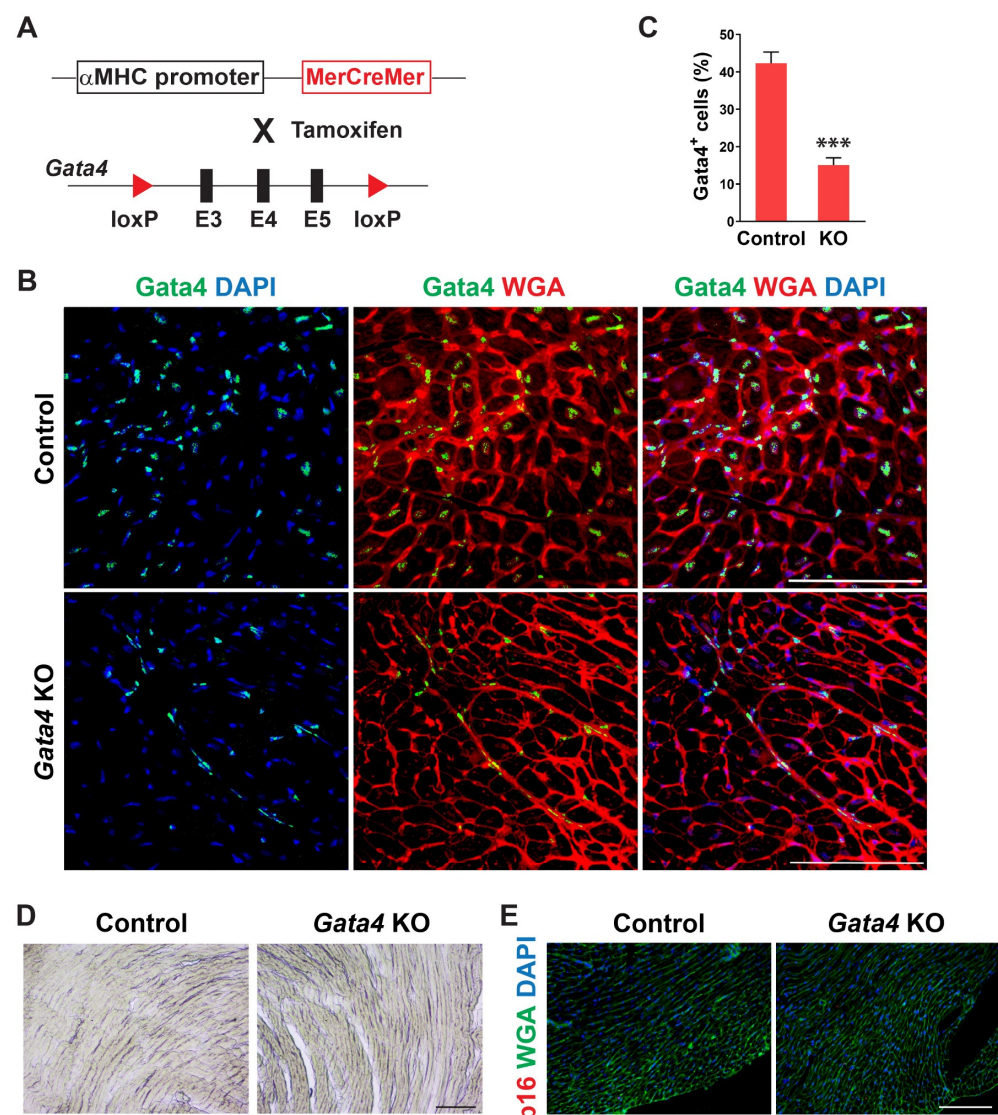


Figure 4. Generation of cardiomyocyte-specific, inducible *Gata4* KO mice and evaluation of senescence induction. (A) Schematic illustration of generation of cardiomyocyte-specific, inducible *Gata4* knockout mice. The transgenic mice which containing α MHC promoter driven *MerCreMer* cDNA cassette and were cross-bred with *Gata4* floxed mice which contained a pair of loxP sites encompassing exons 3, 4, and 5 (E3, 4, and 5). Activated *MerCreMer* by tamoxifen administration recombines two

loxP sites to delete exons 3, 4, and 5 of *Gata4*, thereby inactivating *Gata4* in α MHC lineage traced cardiomyocytes. (B) Immunofluorescent analysis to demonstrate *Gata4* inactivation in α MHC lineage traced cardiomyocytes. A week after tamoxifen administration, α MHC^{iCre} (Control) and α MHC^{iCre}:*Gata4*^{f/f} (*Gata4* KO) mouse hearts were harvested, and heart sections were processed. The heart sections were immunostained for *Gata4* and stained for wheat germ agglutinin (WGA) to demarcate the cell boundary. *Gata4*⁺ nuclei in the WGA-stained interstitial area indicate *Gata4*⁺ interstitial cells. Scale bar, 100 μ M. (C) Quantification of *Gata4*⁺ cells in the heart. *Gata4*⁺DAPI⁺ cells were quantified as *Gata4*⁺ cells in the heart. Three independent experiments are presented as mean \pm s.d. $n = 3$, *** $p < 0.0001$. (D,E) No senescence induction in cardiomyocyte-specific *Gata4* deficient hearts. SA β -gal staining (D) and p16 immunostaining (E) were performed on heart sections 7 weeks following tamoxifen administration into α MHC^{iCre}:*Gata4*^{f/f} (*Gata4* KO) and α MHC^{iCre} (Control) mice. Three mice per group were evaluated. Scale bar, 100 μ M.

4. Discussion

In this study, we demonstrated that genetic disruption of *Gata4* in cardiac fibroblasts spontaneously induces cellular senescence. This result indicates that *Gata4* deficiency in cardiac fibroblasts activates a program of cellular senescence, suggesting a *Gata4*'s senescence-suppressive role in cardiac fibroblasts. However, it seems that *Gata4*'s inhibitory function in cellular senescence is cardiac fibroblast specific, given that we did not observe cellular senescence in a cardiomyocyte-specific *Gata4* deficient mouse model. While the mechanisms underlying senescence induction in response to various cellular stresses have been extensively studied, our understanding of how cellular senescence is controlled in healthy tissues is very limited. Our results provide initial evidence that there is a counter-regulatory mechanism of senescence of cardiac fibroblasts in homeostasis. *Gata4* expression may be necessary to prevent premature cellular senescence in young and healthy cardiac fibroblasts. Markedly decreased *Gata4* expression may prime old cardiac fibroblasts to activate a senescence program upon cellular stresses.

A limitation of our study is that we did not identify the molecular mechanisms underlying senescence induction by loss of *Gata4*. Since *Cdk4* and *Cyclin D2* are direct transcriptional targets of *Gata4* [40,45,50], it can be speculated that these cell cycle proteins may be involved in cardiac fibroblast senescence induced by *Gata4* loss (Figure S6). Understanding how *Gata4* represses the senescence of cardiac fibroblasts may allow us to develop anti-senescence strategies in the future. In addition, the functional significance of senescent cardiac fibroblasts remains elusive. Although we showed an inverse correlation between *Gata4* expression level and the age of mice, our study did not reveal the functional significance of cardiac fibroblast senescence in the uninjured heart. Since cellular senescence has been shown to have both beneficial and detrimental effects [8], it would be interesting to investigate the functional consequence of senescent cardiac fibroblasts in homeostasis.

Kang et al. demonstrated that *Gata4* overexpression spontaneously induces senescence, while *Gata4* knockdown decreases cellular senescence induced by ionizing radiation in IMR-90 human fetal lung and BJ human foreskin fibroblast lines in vitro [51]. Although our results may be in clear contrast with the report from Kang et al., there were a couple of important differences between the previous study and ours. First, the *Gata4* expression level in cardiac fibroblasts is much higher than those derived from other organs [27,28]. It is conceivable that *Gata4* may play differential roles depending on the type of tissues. For example, while *Gata4* in cardiomyocytes is essential for heart development, hypertrophy, and cell survival, cardiomyocyte-specific loss of *Gata4* does not induce senescence. Second, the proliferative capacity of the cells used in our study is much lower than that of human fibroblast lines used in the previous study [51]. Population doubling of IMR-90 and BJ cell lines is about 70–80 times [51–53], while cardiac fibroblasts in the heart are quiescent without injury, and the population doubling of isolated primary cardiac fibroblasts is less than five times in our hands. Collectively, we speculate that *Gata4* may regulate the balance between cell cycle progression and arrest (senescence) depending on proliferative capacity, senescence susceptibility, and/or its expression level in cells.

5. Conclusions

In this work, we defined the role of *Gata4* in cardiac fibroblasts. By using cardiac fibroblast specific *Gata4* knockout mice, we demonstrated that *Gata4* deficiency in cardiac fibroblasts activates a program of cellular senescence. This suggests a novel molecular mechanism of cardiac fibroblast senescence.

Supplementary Materials: The following supporting information can be downloaded at: <https://www.mdpi.com/article/10.3390/cells12121652/s1>, Figure S1: Temporal expression pattern of *Gata4* in the heart; Figure S2: Non-myocytes from *Tcf21iCre:R26RtdT* (Control) and *Tcf21iCre:Gata4^{fl/fl}:R26RtdT* (*Gata4* KO) mice; Figure S3: Senescence induction in *Gata4* deficient cardiac fibroblasts in vitro; Figure S4: Generation of cardiomyocyte-specific, inducible *Gata4* KO mice; Figure S5: *Tcf21^{iCre}:Gata4^{fl/fl}*, and α MHC^{iCre}:*Gata4^{fl/fl}* and WT mice were examined by transthoracic echocardiogram; Figure S6: Assessing expression levels of Cdk4 and Cyclin D2 following the loss of *Gata4* in cardiac fibroblasts; Table S1: Sequence of primers used for RT-PCR studies.

Author Contributions: Conceptualization, Z.Z.; methodology, Z.Z., H.F. and Y.H.; formal analysis, Z.Z.; investigation, Z.Z., H.F., G.S., A.K. and Y.H.; data curation, Z.Z. and H.Z., Y.X.; writing—original draft, Z.Z., H.Z. and Y.X.; writing—review and editing, all authors; funding acquisition, Z.Z. and H.Z. All authors have read and agreed to the published version of the manuscript.

Funding: This work was supported by Gilead Sciences Research Scholars Program and NIH (R01 HL146524), NIH (R01 HL153876), AHA (20POST35210170), AHA (23CDA1045959).

Institutional Review Board Statement: Not applicable. The study was conducted according to the guidelines of the Declaration of Helsinki, and approved by the Institutional Review Board of Vanderbilt University Medical Center (Protocol No. M1700064-01).

Informed Consent Statement: Not applicable.

Data Availability Statement: The original contributions presented in this study are included in the article. Further inquiries can be directed to the corresponding author.

Acknowledgments: High-content imaging analysis was performed in the Vanderbilt High-Throughput Screening (HTS) Core Facility. The HTS Core receives support from the Vanderbilt Institute of Chemical Biology and the Vanderbilt Ingram Cancer Center (P30 CA68485).

Conflicts of Interest: The authors declare that the research was conducted without any commercial or financial relationships that could be construed as a potential conflict of interest.

References

1. Souders, C.A.; Bowers, S.L.; Baudino, T.A. Cardiac fibroblast: The renaissance cell. *Circ. Res.* **2009**, *105*, 1164–1176. [CrossRef]
2. Travers, J.G.; Kamal, F.A.; Robbins, J.; Yutzey, K.E.; Blaxall, B.C. Cardiac Fibrosis: The Fibroblast Awakens. *Circ. Res.* **2016**, *118*, 1021–1040. [CrossRef]
3. Spinale, F.G. Myocardial matrix remodeling and the matrix metalloproteinases: Influence on cardiac form and function. *Physiol. Rev.* **2007**, *87*, 1285–1342. [CrossRef]
4. Weber, K.T.; Sun, Y.; Bhattacharya, S.K.; Ahokas, R.A.; Gerling, I.C. Myofibroblast-mediated mechanisms of pathological remodeling of the heart. *Nat. Rev. Cardiol.* **2013**, *10*, 15–26. [CrossRef]
5. Munoz-Espin, D.; Serrano, M. Cellular senescence: From physiology to pathology. *Nat. Rev. Mol. Cell Biol.* **2014**, *15*, 482–496. [CrossRef]
6. Gorgoulis, V.; Adams, P.D.; Alimonti, A.; Bennett, D.C.; Bischof, O.; Bishop, C.; Campisi, J.; Collado, M.; Evangelou, K.; Ferbeyre, G.; et al. Cellular Senescence: Defining a Path Forward. *Cell* **2019**, *179*, 813–827. [CrossRef] [PubMed]
7. Herranz, N.; Gil, J. Mechanisms and functions of cellular senescence. *J. Clin. Investig.* **2018**, *128*, 1238–1246. [CrossRef] [PubMed]
8. Rhinn, M.; Ritschka, B.; Keyes, W.M. Cellular senescence in development, regeneration and disease. *Development* **2019**, *146*, dev151837. [CrossRef] [PubMed]
9. Krizhanovsky, V.; Yon, M.; Dickins, R.A.; Hearn, S.; Simon, J.; Miething, C.; Yee, H.; Zender, L.; Lowe, S.W. Senescence of activated stellate cells limits liver fibrosis. *Cell* **2008**, *134*, 657–667. [CrossRef] [PubMed]
10. Jun, J.I.; Lau, L.F. The matricellular protein CCN1 induces fibroblast senescence and restricts fibrosis in cutaneous wound healing. *Nat. Cell Biol.* **2010**, *12*, 676–685. [CrossRef] [PubMed]
11. Demaria, M.; Ohtani, N.; Youssef, S.A.; Rodier, F.; Toussaint, W.; Mitchell, J.R.; Laberge, R.-M.; Vijg, J.; Van Steeg, H.; Dollé, M.E.; et al. An essential role for senescent cells in optimal wound healing through secretion of PDGF-AA. *Dev. Cell* **2014**, *31*, 722–733. [CrossRef] [PubMed]

12. Schafer, M.J.; White, T.A.; Iijima, K.; Haak, A.J.; Ligresti, G.; Atkinson, E.J.; Oberg, A.L.; Birch, J.; Salmonowicz, H.; Zhu, Y.; et al. Cellular senescence mediates fibrotic pulmonary disease. *Nat. Commun.* **2017**, *8*, 14532. [[CrossRef](#)] [[PubMed](#)]
13. Zhu, F.; Li, Y.; Zhang, J.; Piao, C.; Liu, T.; Li, H.-H.; Du, J. Senescent cardiac fibroblast is critical for cardiac fibrosis after myocardial infarction. *PLoS ONE* **2013**, *8*, e74535. [[CrossRef](#)]
14. Meyer, K.; Hodwin, B.; Ramanujam, D.; Engelhardt, S.; Sarikas, A. Essential Role for Premature Senescence of Myofibroblasts in Myocardial Fibrosis. *J. Am. Coll. Cardiol.* **2016**, *67*, 2018–2028. [[CrossRef](#)] [[PubMed](#)]
15. Shibamoto, M.; Higo, T.; Naito, A.T.; Nakagawa, A.; Sumida, T.; Okada, K.; Sakai, T.; Kuramoto, Y.; Yamaguchi, T.; Ito, M.; et al. Activation of DNA Damage Response and Cellular Senescence in Cardiac Fibroblasts Limit Cardiac Fibrosis after Myocardial Infarction. *Int. Heart J.* **2019**, *60*, 944–957. [[CrossRef](#)]
16. Dookun, E.; Walaszczyk, A.; Redgrave, R.; Palmowski, P.; Tual-Chalot, S.; Suwana, A.; Chapman, J.; Jirkovsky, E.; Sosa, L.D.; Gill, E.; et al. Clearance of senescent cells during cardiac ischemia-reperfusion injury improves recovery. *Aging Cell* **2020**, *19*, e13249. [[CrossRef](#)]
17. Paramos-de-Carvalho, D.; Martins, I.; Cristóvão, A.M.; Dias, A.F.; Neves-Silva, D.; Pereira, T.; Chapela, D.; Farinho, A.; Jacinto, A.; Saúde, L. Targeting senescent cells improves functional recovery after spinal cord injury. *Cell Rep.* **2021**, *36*, 109334. [[CrossRef](#)]
18. Arceci, R.J.; King, A.A.J.; Simon, M.C.; Orkin, S.H.; Wilson, D.B. Mouse GATA-4: A retinoic acid-inducible GATA-binding transcription factor expressed in endodermally derived tissues and heart. *Mol. Cell Biol.* **1993**, *13*, 2235–2246.
19. Aries, A.; Paradis, P.; Lefebvre, C.; Schwartz, R.J.; Nemer, M. Essential role of GATA-4 in cell survival and drug-induced cardiotoxicity. *Proc. Natl. Acad. Sci. USA* **2004**, *101*, 6975–6980. [[CrossRef](#)]
20. Charron, F.; Tsimiklis, G.; Arcand, M.; Robitaille, L.; Liang, Q.; Molkentin, J.D.; Meloche, S.; Nemer, M. Tissue-specific GATA factors are transcriptional effectors of the small GTPase RhoA. *Genes Dev.* **2001**, *15*, 2702–2719. [[CrossRef](#)]
21. Kuo, C.T.; Morrisey, E.E.; Anandappa, R.; Sigrist, K.; Lu, M.M.; Parmacek, M.S.; Soudais, C.; Leiden, J.M. GATA4 transcription factor is required for ventral morphogenesis and heart tube formation. *Genes Dev.* **1997**, *11*, 1048–1060. [[CrossRef](#)] [[PubMed](#)]
22. Liang, Q.; De Windt, L.J.; Witt, S.A.; Kimball, T.R.; Markham, B.E.; Molkentin, J.D. The transcription factors GATA4 and GATA6 regulate cardiomyocyte hypertrophy in vitro and in vivo. *J. Biol. Chem.* **2001**, *276*, 30245–30253. [[CrossRef](#)]
23. Molkentin, J.D. The zinc finger-containing transcription factors GATA-4, -5, and -6. Ubiquitously expressed regulators of tissue-specific gene expression. *J. Biol. Chem.* **2000**, *275*, 38949–38952. [[CrossRef](#)] [[PubMed](#)]
24. Molkentin, J.D.; Lin, Q.; Duncan, S.A.; Olson, E.N. Requirement of the transcription factor GATA4 for heart tube formation and ventral morphogenesis. *Genes Dev.* **1997**, *11*, 1061–1072. [[CrossRef](#)] [[PubMed](#)]
25. Monzen, K.; Shiojima, I.; Hiroi, Y.; Kudoh, S.; Oka, T.; Takimoto, E.; Hayashi, D.; Hosoda, T.; Habara-Ohkubo, A.; Nakaoka, T.; et al. Bone morphogenetic proteins induce cardiomyocyte differentiation through the mitogen-activated protein kinase kinase TAK1 and cardiac transcription factors Csx/Nkx-2.5 and GATA-4. *Mol. Cell Biol.* **1999**, *19*, 7096–7105. [[CrossRef](#)]
26. Boheler, K.R.; Czyn, J.; Tweedie, D.; Yang, H.-T.; Anisimov, S.V.; Wobus, A.M. Differentiation of pluripotent embryonic stem cells into cardiomyocytes. *Circ. Res.* **2002**, *91*, 189–201. [[CrossRef](#)]
27. Furtado, M.B.; Costa, M.; Pranoto, E.A.; Salimova, E.; Pinto, A.R.; Lam, N.; Park, A.; Snider, P.; Chandran, A.; Harvey, R.; et al. Cardiogenic genes expressed in cardiac fibroblasts contribute to heart development and repair. *Circ. Res.* **2014**, *114*, 1422–1434. [[CrossRef](#)]
28. Zaglia, T.; Dedja, A.; Candiotti, C.; Cozzi, E.; Schiaffino, S.; Ausoni, S. Cardiac interstitial cells express GATA4 and control differentiation and cell cycle re-entry of adult cardiomyocytes. *J. Mol. Cell Cardiol.* **2009**, *46*, 653–662. [[CrossRef](#)]
29. Dittrich, G.M.; Froese, N.; Wang, X.; Kroeger, H.; Wang, H.; Szaroszyk, M.; Malek-Mohammadi, M.; Cordero, J.; Keles, M.; Korf-Klingebiel, M.; et al. Fibroblast GATA-4 and GATA-6 promote myocardial adaptation to pressure overload by enhancing cardiac angiogenesis. *Basic Res. Cardiol.* **2021**, *116*, 26. [[CrossRef](#)]
30. Acharya, A.; Baek, S.T.; Banfi, S.; Eskiocak, B.; Tallquist, M.D. Efficient inducible Cre-mediated recombination in Tcf21 cell lineages in the heart and kidney. *Genesis* **2011**, *49*, 870–877. [[CrossRef](#)]
31. Song, K.; Nam, Y.-J.; Luo, X.; Qi, X.; Tan, W.; Huang, G.N.; Acharya, A.; Smith, C.L.; Tallquist, M.D.; Neilson, E.G.; et al. Heart repair by reprogramming non-myocytes with cardiac transcription factors. *Nature* **2012**, *485*, 599–604. [[CrossRef](#)]
32. Watt, A.J.; Battle, M.A.; Li, J.; Duncan, S.A. GATA4 is essential for formation of the proepicardium and regulates cardiogenesis. *Proc. Natl. Acad. Sci. USA* **2004**, *101*, 12573–12578. [[CrossRef](#)] [[PubMed](#)]
33. O’Connell, T.D.; Rodrigo, M.C.; Simpson, P.C. Isolation and culture of adult mouse cardiac myocytes. *Methods Mol. Biol.* **2007**, *357*, 271–296. [[PubMed](#)]
34. Zhang, Z.; Nam, Y.J. Assessing Cardiac Reprogramming using High Content Imaging Analysis. *J. Vis. Exp.* **2020**, *164*, e61859.
35. Zhang, Z.; Villalpando, J.; Zhang, W.; Nam, Y.-J. Chamber-Specific Protein Expression during Direct Cardiac Reprogramming. *Cells* **2021**, *10*, 1513. [[CrossRef](#)] [[PubMed](#)]
36. Zhang, Z.; Zhang, A.D.; Kim, L.J.; Nam, Y.-J. Ensuring expression of four core cardiogenic transcription factors enhances cardiac reprogramming. *Sci. Rep.* **2019**, *9*, 6362. [[CrossRef](#)]
37. Zhang, Z.; Zhang, W.; Nam, Y.J. Stoichiometric optimization of Gata4, Hand2, Mef2c, and Tbx5 expression for contractile cardiomyocyte reprogramming. *Sci. Rep.* **2019**, *9*, 14970. [[CrossRef](#)]
38. Moore-Morris, T.; Guimarães-Camboa, N.; Banerjee, I.; Zambon, A.C.; Kisseleva, T.; Velayoudon, A.; Stallcup, W.B.; Gu, Y.; Dalton, N.D.; Cedenilla, M.; et al. Resident fibroblast lineages mediate pressure overload-induced cardiac fibrosis. *J. Clin. Investig.* **2014**, *124*, 2921–2934. [[CrossRef](#)]

39. Ali, S.R.; Ranjbarvaziri, S.; Talkhabi, M.; Zhao, P.; Subat, A.; Hojjat, A.; Kamran, P.; Müller, A.M.; Volz, K.S.; Tang, Z.; et al. Developmental heterogeneity of cardiac fibroblasts does not predict pathological proliferation and activation. *Circ. Res.* **2014**, *115*, 625–635. [[CrossRef](#)]
40. Rojas, A.; Kong, S.W.; Agarwal, P.; Gilliss, B.; Pu, W.T.; Black, B.L. GATA4 is a direct transcriptional activator of cyclin D2 and Cdk4 and is required for cardiomyocyte proliferation in anterior heart field-derived myocardium. *Mol. Cell Biol.* **2008**, *28*, 5420–5431. [[CrossRef](#)]
41. Kohlnhofer, B.M.; Thompson, C.A.; Walker, E.M.; Battle, M.A. GATA4 regulates epithelial cell proliferation to control intestinal growth and development in mice. *Cell Mol. Gastroenterol. Hepatol.* **2016**, *2*, 189–209. [[CrossRef](#)]
42. Yao, C.-X.; Shi, J.-C.; Ma, C.-X.; Xiong, C.-J.; Song, Y.-L.; Zhang, S.-F.; Zhang, S.-F.; Zang, M.-X.; Xue, L.-X. EGF Protects Cells Against Dox-Induced Growth Arrest Through Activating Cyclin D1 Expression. *J. Cell Biochem.* **2015**, *116*, 1755–1765. [[CrossRef](#)]
43. Yao, C.-X.; Wei, Q.-X.; Zhang, Y.-Y.; Wang, W.-P.; Xue, L.-X.; Yang, F.; Zhang, S.-F.; Xiong, C.-J.; Li, W.-Y.; Wei, Z.-R.; et al. miR-200b targets GATA-4 during cell growth and differentiation. *RNA Biol.* **2013**, *10*, 465–480. [[CrossRef](#)]
44. Kyronlahti, A.; Ramo, M.; Tamminen, M.; Unkila-Kallio, L.; Butzow, R.; Leminen, A.; Nemer, M.; Rahman, N.; Huhtaniemi, I.; Heikinheimo, M.; et al. GATA-4 regulates Bcl-2 expression in ovarian granulosa cell tumors. *Endocrinology* **2008**, *149*, 5635–5642. [[CrossRef](#)]
45. Yamak, A.; Temsah, R.; Maharsy, W.; Caron, S.; Paradis, P.; Aries, A.; Nemer, M. Cyclin D₂ rescues size and function of GATA4 haplo-insufficient hearts. *Am. J. Physiol. Heart Circ. Physiol.* **2012**, *303*, H1057–H1066. [[CrossRef](#)]
46. Trivedi, C.M.; Zhu, W.; Wang, Q.; Jia, C.; Kee, H.J.; Li, L.; Hannenhalli, S.; Epstein, J.A. Hopx and Hdac2 interact to modulate Gata4 acetylation and embryonic cardiac myocyte proliferation. *Dev. Cell* **2010**, *19*, 450–459. [[CrossRef](#)]
47. Han, Q.; Xu, X.; Li, J.; Wang, J.; Bai, L.; Wang, A.; Wang, W.; Zhang, B. GATA4 is highly expressed in childhood acute lymphoblastic leukemia, promotes cell proliferation and inhibits apoptosis by activating BCL2 and MDM2. *Mol. Med. Rep.* **2017**, *16*, 6290–6298. [[CrossRef](#)] [[PubMed](#)]
48. Hernandez-Segura, A.; Nehme, J.; Demaria, M. Hallmarks of Cellular Senescence. *Trends Cell Biol.* **2018**, *28*, 436–453. [[CrossRef](#)]
49. Sohal, D.S.; Nghiem, M.; Crackower, M.A.; Witt, S.A.; Kimball, T.R.; Tymitz, K.M.; Penninger, J.M.; Molkenkin, J.D. Temporally regulated and tissue-specific gene manipulations in the adult and embryonic heart using a tamoxifen-inducible Cre protein. *Circ. Res.* **2001**, *89*, 20–25. [[CrossRef](#)] [[PubMed](#)]
50. Yamak, A.; Latinkić, B.V.; Dali, R.; Temsah, R.; Nemer, M. Cyclin D₂ is a GATA4 cofactor in cardiogenesis. *Proc. Natl. Acad. Sci. USA* **2014**, *111*, 1415–1420. [[CrossRef](#)] [[PubMed](#)]
51. Kang, C.; Xu, Q.; Martin, T.D.; Li, M.Z.; DeMaria, M.; Aron, L.; Lu, T.; Yankner, B.A.; Campisi, J.; Elledge, S.J. The DNA damage response induces inflammation and senescence by inhibiting autophagy of GATA4. *Science* **2015**, *349*, aaa5612. [[CrossRef](#)] [[PubMed](#)]
52. Nichols, W.W.; Murphy, D.G.; Cristofalo, V.J.; Toji, L.H.; Greene, A.E.; Dwight, S.A. Characterization of a new human diploid cell strain, IMR-90. *Science* **1977**, *196*, 60–63. [[CrossRef](#)] [[PubMed](#)]
53. Morales, C.P.; Holt, S.E.; Ouellette, M.; Kaur, K.J.; Yan, Y.; Wilson, K.S.; White, M.A.; Wright, W.E.; Shay, J.W. Absence of cancer-associated changes in human fibroblasts immortalized with telomerase. *Nat. Genet.* **1999**, *21*, 115–118. [[CrossRef](#)] [[PubMed](#)]

Disclaimer/Publisher’s Note: The statements, opinions and data contained in all publications are solely those of the individual author(s) and contributor(s) and not of MDPI and/or the editor(s). MDPI and/or the editor(s) disclaim responsibility for any injury to people or property resulting from any ideas, methods, instructions or products referred to in the content.